



UvA-DARE (Digital Academic Repository)

The biogeographic and evolutionary processes shaping population divergence in *Laupala*

Blankers, T.; Shaw, K.L.

DOI

[10.1111/mec.17444](https://doi.org/10.1111/mec.17444)

Publication date

2024

Document Version

Final published version

Published in

Molecular Ecology

License

CC BY-NC

[Link to publication](#)

Citation for published version (APA):

Blankers, T., & Shaw, K. L. (2024). The biogeographic and evolutionary processes shaping population divergence in *Laupala*. *Molecular Ecology*, 33(15), Article e17444. <https://doi.org/10.1111/mec.17444>

General rights

It is not permitted to download or to forward/distribute the text or part of it without the consent of the author(s) and/or copyright holder(s), other than for strictly personal, individual use, unless the work is under an open content license (like Creative Commons).

Disclaimer/Complaints regulations

If you believe that digital publication of certain material infringes any of your rights or (privacy) interests, please let the Library know, stating your reasons. In case of a legitimate complaint, the Library will make the material inaccessible and/or remove it from the website. Please Ask the Library: <https://uba.uva.nl/en/contact>, or a letter to: Library of the University of Amsterdam, Secretariat, P.O. Box 19185, 1000 GD Amsterdam, The Netherlands. You will be contacted as soon as possible.

UvA-DARE is a service provided by the library of the University of Amsterdam (<https://dare.uva.nl>)

The biogeographic and evolutionary processes shaping population divergence in *Laupala*

Thomas Blankers^{1,2}  | Kerry L. Shaw¹

¹Department of Neurobiology and Behavior, Cornell University, Ithaca, New York, USA

²Institute for Biodiversity and Ecosystem Dynamics, University of Amsterdam, Amsterdam, The Netherlands

Correspondence

Thomas Blankers and Kerry L. Shaw, Institute for Biodiversity and Ecosystem Dynamics, University of Amsterdam, Science Park 904, 1098XH, Amsterdam, The Netherlands.
Email: t.blankers@uva.nl and kls4@cornell.edu

Funding information

National Science Foundation, Grant/Award Number: DEB1241060

Handling Editor: Brent Emerson

Abstract

Speciation generates biodiversity and the mechanisms involved are thought to vary across the tree of life and across environments. For example, well-studied adaptive radiations are thought to be fuelled by divergent ecological selection, but additionally are influenced heavily by biogeographic, genomic and demographic factors. Mechanisms of non-adaptive radiations, producing ecologically cryptic taxa, have been less well-studied but should likewise be influenced by these latter factors. Comparing among contexts can help pinpoint universal mechanisms and outcomes, especially if we integrate biogeographic, ecological and evolutionary processes. We investigate population divergence in the swordtail cricket *Laupala cerasina*, a widespread endemic on Hawai'i Island and one of 38 ecologically cryptic *Laupala* species. The nine sampled populations show striking population genetic structure at small spatio-temporal scales. The rapid differentiation among populations and species of *Laupala* shows that neither a specific geographical context nor ecological opportunity are pre-requisites for rapid divergence. Spatio-temporal patterns in population divergence, population size change, and gene flow are aligned with the chronosequence of the four volcanoes on which *L. cerasina* occurs and reveal the composite effects of geological dynamics and Quaternary climate change on population dynamics. Spatio-temporal patterns in genetic variation along the genome reveal the interplay of genetic and genomic architecture in shaping population divergence. In early phases of divergence, we find elevated differentiation in genomic regions harbouring mating song loci. In later stages of divergence, we find a signature of linked selection that interacts with recombination rate variation. Comparing our findings with recent work on complementary systems supports the conclusion that mostly universal factors influence the speciation process.

KEYWORDS

biogeography, genomics, *Laupala*, non-adaptive radiation, speciation

This is an open access article under the terms of the [Creative Commons Attribution-NonCommercial](https://creativecommons.org/licenses/by-nc/4.0/) License, which permits use, distribution and reproduction in any medium, provided the original work is properly cited and is not used for commercial purposes.

© 2024 The Author(s). *Molecular Ecology* published by John Wiley & Sons Ltd.

1 | INTRODUCTION

Speciation is a complex process that occurs in widely different geographical, ecological and spatio-temporal contexts, with studies often focusing on particular mechanisms that are considered important in a given context. To identify universal mechanisms that might underpin speciation, we must integrate across a range of evolutionary, ecological, biogeographic and geological mechanisms that can influence the speciation process. A contrast between adaptive radiations and non-adaptive radiations may promise such insights. Adaptive radiations have long drawn the interest of evolutionary biologists due to their ecological diversity, convergent evolution and rapid rates of speciation (Gillespie et al., 2020). In contrast, non-adaptive species radiations are less well-studied, despite making up a significant component of biodiversity, especially cryptic biodiversity (Czekanski-Moir & Rundell, 2019; Rundell & Price, 2009; Simões et al., 2016). The distinctive outcome of a non-adaptive radiation is a phylogenetic cluster of closely related species that share, rather than differ in, ecological attributes such as mechanisms of resource acquisition or predator defence (although such differences could evolve subsequently). One of the more conspicuous forms of non-adaptive radiation occurs when species vary in traits involved in mating and/or fertilisation.

Like adaptive radiations, speciation in non-adaptive radiations may also occur rapidly (Czekanski-Moir & Rundell, 2019; Rundell & Price, 2009), promising insights into their similarities as opposed to their differences. For example, contrasting adaptive with non-adaptive radiations can suggest a crucial role for selection in rapid species radiations, with differing biological outcomes depending on the selection mechanisms involved. It is commonly emphasised that divergent ecological selection is the central driving force behind adaptive radiation (Gavrilets & Losos, 2009; Gillespie et al., 2020; Nosil & Schluter, 2011; Schluter, 1996, 2000). Likewise, rapid non-adaptive radiation resulting in species that differ in, for example, sexual signalling traits suggests divergent sexual selection as a central driving force. In either case, barriers to gene exchange that foster genetic isolation among resulting species arise due to divergent selection favouring variants that eventually characterise daughter species. This perspective on the origins of species radiations directs our attention toward understanding the mechanisms of selection that promote trait evolution causing barriers to gene exchange. Further, such a perspective suggests that swapping one form of selection for another, results in vital distinctions between different forms of species radiations.

It is increasingly being recognised that a multitude of factors in addition to selection influence the evolution of reproductive barriers and shape evolutionary outcomes of speciation, many of which adaptive and non-adaptive radiations might be expected to share. The accumulation of genetic divergence among populations, integral to the speciation process, illustrates this complexity quite well. On the one hand, selection acting on specific traits (e.g. as discussed above) and their underlying genetic architecture, mediated by the genomic and recombination landscape, can result in heterogeneous

divergence across the genome (Burri et al., 2015; Marques et al., 2016; Martin et al., 2013; Stankowski et al., 2019). Conversely, factors such as biogeography and demography (e.g. arising from dispersal capacity of the organism and population size) should influence divergence of the genome as a whole. This constellation of factors influencing divergence is further complicated by the counteracting effects of gene flow, as illustrated by taxa diverging in the face of relatively high gene flow, such as *Heliconius* butterflies (Martin et al., 2013), cichlids (Malinsky et al., 2018; Meier et al., 2017) and monkeyflowers (Stankowski et al., 2019), and others diverging with relatively low levels of gene flow, such as *Begonia* plants (Twyford et al., 2015), *Pyramidula* snails (Razkin et al., 2016) and Hawaiian stick spiders (Armstrong et al., 2021). Thus, while adaptive radiations differ from non-adaptive ones in the presence of ecological selection, both types of radiations exhibit genetic divergence over time, involving selection and genetic drift, mediated by genome dynamics, demography and biogeographic landscapes. Given these important features that play a role in speciation, it is conceivable that the ways in which adaptive and non-adaptive radiations are similar far outnumber the ways in which they differ. Examining the mechanisms underlying each type of radiation will be necessary to evaluate unexpected suggestions such as high(er) rates of speciation in nonadaptive radiations (Kozak et al., 2006; Mendelson & Shaw, 2005), or initial non-adaptive phases to adaptive radiations (Cotoras et al., 2018), which may be a common pattern in vertebrate speciation (Anderson & Weir, 2022).

In this study, we examined the earliest stages of a non-adaptive radiation, as represented by the swordtail cricket *Laupala cerasina*. Specifically, we compare the influence of biogeography to that of evolutionary mechanisms and genomic constraints, to gain insight into the intraspecific evolutionary processes that have given rise to a non-adaptive radiation. The genus *Laupala* is hypothesised to be a non-adaptive radiation, due to divergent mating behaviours among closely related species coupled with morphological and ecological cypsis (Grace & Shaw, 2011, 2012; Mendelson & Shaw, 2002; Otte, 1994). The radiation is entirely endemic to the Hawaiian archipelago and shows a strong biogeographic signature known as the 'progression rule' (Funk & Wagner, 1995; Hennig, 1966), wherein the timing and branching of clades are concordant with the sequential ages of land areas in which they reside. In *Laupala*, phylogenetic patterns indicate a radiation that began on older volcanic islands and diversified to younger islands, as they became available (Mendelson & Shaw, 2005; Shaw & Gillespie, 2016). *Laupala cerasina* is endemic to Hawai'i Island, the youngest island in the archipelago, and thus one of the youngest lineages of this non-adaptive radiation. Like other species of the genus, *L. cerasina* are flightless and small (~1 cm) and typically found in mid-elevation 'Ōhi'a - Hāpu'u' rainforest dominated by *Metrosideros polymorpha* and *Citobium glaucum*.

We first assessed the biogeographic processes that shaped the evolutionary history of *L. cerasina*. The geology of Hawai'i is highly dynamic. The four volcanos on which *L. cerasina* can be found emerged above sea level in chronosequence: Kohala 430 thousand years ago (ka), Mauna Kea 380ka, Mauna Loa 200ka and Kilauea

100 ka (Porter, 2005; Roderick et al., 2012). The interaction between Quaternary climate fluctuations, rising volcanoes and recurrent lava flows would have continuously shaped the available *L. cerasina* habitat throughout the last 500,000 years (Hotchkiss & Juvik, 1999; Izuno et al., 2022). We hypothesised a population genetic structure in *L. cerasina* reflecting these landscape dynamics, with a distinct signature of the chronosequence due to fluctuating habitat availability and fragmented landscapes as volcano summits rose and vegetation zones shifted in response to the changing climate. This signature of chronosequence should exhibit substantial similarity to a progression rule phylogeographic pattern observed across *Laupala* and many other island organisms (Funk & Wagner, 1995; Hembry et al., 2021; Shaw & Gillespie, 2016).

To test this hypothesis, we used spatially explicit, phylogeographic and population genetic analyses, by considering four putative population structures in *L. cerasina*: (1) *L. cerasina* is an interconnected meta-population and sub-populations have only very recently become separated, (2) *L. cerasina* populations were shaped by extinction-recolonisation dynamics due to repeated lava flows dissecting the landscape, obliterating older forests and creating newer substrates in support of younger forests, (3) *L. cerasina* populations were established by progressive founder events following the volcanic chronosequence and subsequent origin of forest habitat, (4) populations established by (gradual) range expansion and were subsequently fragmented. Under scenario 1 we would expect a strong relationship between geographical distance and genetic differentiation, known as isolation by distance (IBD) (Slatkin, 1993) and high levels of gene flow among more geographically proximate populations. In particular, this scenario does not predict genetic and demographic signatures of the geologic chronology of the island. Under scenario 2 and 3, we expect signatures of genetic bottlenecks and stronger genetic distinctions among subpopulations relative to scenario 1. In addition, scenario 2 would suggest higher genetic differentiation among more recently established populations compared to older populations that have subsequently re-established contact through migration (Angst et al., 2022; Pannell & Charlesworth, 2000). Scenario 3 predicts a progression pattern, concordance between population divergence times and volcanic ages and increasing F_{ST} between *L. cerasina* populations on younger volcanoes, and *L. waikemoi*, a closely related species to *L. cerasina* on the neighbouring island of Maui (Funk & Wagner, 1995; Hennig, 1966; Shaw & Gillespie, 2016). Scenario 4 similarly predicts a correspondence between population divergence times and volcano age due to the sequential effects of rising adjacent volcanoes or erosional dynamics on extinct volcanoes on forest habitat fragmentation. In contrast to scenario 3 (and 2), a signature of bottlenecks would not be expected under scenario 4.

Within the observed biogeographic pattern, we next examined molecular variation across the genomes of *L. cerasina* populations. We focus on the relationship between measures of genetic difference, the genomic landscape of recombination and the genetic architecture of traits important in *Laupala* speciation to identify evolutionary processes shaping the earliest stages of divergence. Prior

evidence suggested that populations have diverged predominantly in allopatry (Mendelson et al., 2004) and thus we hypothesised a negative correlation between population differentiation (F_{ST}) and recombination rate (Nachman & Payseur, 2012). This is because, in regions of low recombination, the loss of genetic diversity due to the effects of linked selection (purifying selection plus positive selection) affects larger genomic intervals compared to in regions of high recombination. We further expect the strength of the relationship between F_{ST} and recombination rate to increase as divergence time increases (Burri, 2017; Matthey-Doret & Whitlock, 2019). Conversely, dxy , a measure of absolute nucleotide divergence, mostly reflects within-population nucleotide diversity early in the divergence process. Due to the reduction in diversity, linked selection should reduce dxy more strongly in regions of low recombination relative to the genome-wide average (Nachman & Payseur, 2012), but this signature is expected to become less pronounced with time since divergence. Under a divergence-with-gene flow scenario, dxy is expected to be more reduced in regions of high recombination (Nachman & Payseur, 2012), but may still reveal positive genome-wide correlations with recombination rate as the effect of linked selection is likely to be more widespread than that of gene flow (e.g. Stankowski et al., 2019).

A defining feature of both adaptive and non-adaptive radiations is the rapid evolution of reproductive barriers. Since there are modest but statistically significant differences in the male song and female preferences among populations of *L. cerasina* that show early effects on mating compatibility (Grace & Shaw, 2011, 2012), we asked if regions in the genome known to be associated with song differences among species showed elevated divergence early on or throughout the divergence process. It is generally expected that populations show greater differentiation (F_{ST}) and, given enough time has passed for genetic differences to accumulate, also greater absolute divergence (dxy) close to loci where selection acts against gene flow or where selection favours locally adaptive alleles (Burri, 2017; Ravinet et al., 2017). Similar effects may be expected for the loci underlying divergent sexual communication behaviours. When reproductive barriers evolve rapidly, in the absence of ecological differences, divergence in sexual communication can leave clear signatures in the genome (Campagna et al., 2017; Toews et al., 2016), although this will depend on the number of loci involved and their relative effect sizes.

We recently assembled the *Laupala* genome into pseudomolecules, inferred recombination rate variation across the genome (Blankers, Oh, Bombarely, et al., 2018), and identified quantitative trait loci (QTL) underlying song divergence between *L. cerasina* and the closely related *L. eukolea* (Blankers, Oh, & Shaw, 2018). Here, we use these newly developed resources and generate genotype-by-sequencing loci for 186 new individuals. We test for the presence of population genetic structure and relate patterns in population structure to the geology and biogeography of the island. We then examine the effects of population size variation and gene flow on population divergence, and ask whether genomic regions containing song QTL harboured disproportionate

amounts of genetic divergence among populations. We go on to discuss these findings in the light of other population or species radiations with or without gene flow and with or without ecological differentiation.

2 | METHODS

2.1 | Samples

We sampled *L. cerasina* males and females between 2015 and 2017 at nine different locations on Hawai'i Island (Table S1, Figure 1a). A total of 165 *L. cerasina* were collected. One individual was excluded because preliminary analyses indicated it was wrongly classified as belonging to the Kalopa Park population. We also collected 11 females and 10 males belonging to *L. waikemoi* from Waikemoi, East Maui as outgroup data and to facilitate contrasting intraspecific versus interspecific levels of divergence. We checked for relatedness based on the KING inference (Manichaikul et al., 2010) using the option `-relatedness2` in VCFtools 0.1.15 (Danecek et al., 2011) and found two half-sibs ($0.09 < \varphi < 0.18$) and one full sib ($0.18 < \varphi < 0.35$) pair. Each pair was in a different population (Ponoholo, Laupahoehoe, Lorenzo Rd). None of these individuals were removed for subsequent analysis.

2.2 | Genotyping

We extracted DNA from whole individuals, then sequenced individual libraries using Genotype-By-Sequencing at the Genomic Diversity Facility at Cornell University following Elshire et al. (2011). The PstI restriction enzyme was used and DNA was sequenced (1×100 bp) on the Illumina HiSeq2000 platform. We processed multiplexed reads following the protocols and using the *L. kohalensis* draft assembly (described in Blankers, Oh, Bombarely, et al., 2018) retaining on average 1,872,035 reads per individual after filtering.

Single nucleotide polymorphisms (SNPs) were called and then filtered using stringent cut-offs for depth and sequencing quality independently in two different SNP-calling pipelines, FreeBayes 0.9.13 (Garrison & Marth, 2012) and GATK 3.6.0 (DePristo et al., 2011; Van der Auwera et al., 2013). The FreeBayes (159,268 before filtering; 95,063 after filtering) and GATK (198,304 before filtering; 19,659 after filtering) variant call files (VCF) were then merged and only SNPs with more than 95% identical genotypes between the variant callers were retained after which files were processed further in VCFtools to remove SNPs with high rates of missing information ($>10\%$) or that were less than 50kbp apart (retaining 4794 variants). Unless specified otherwise, a minor allele count of 1 was used, meaning singletons are present in the data set. The rationale here is that our filtering strategies provide confidence in the SNP calls and additional minor allele frequency cut-offs would more likely remove true rare variants rather than false positive variants. For questions that addressed genome-wide patterns of variation among the populations, we used the full set of 4794 SNPs that was obtained as described above. To look at patterns of variation within the genome, we mapped our SNPs to the *L. kohalensis* pseudo-molecule assembly (2797 variants), thus omitting SNPs not mapping to scaffolds previously assembled into linkage groups (Blankers, Oh, Bombarely, et al., 2018). See the Supplementary methods on SNP selection for more details.

2.3 | Population structure

Laupala cerasina is distributed broadly across the eastern side of Hawai'i Island (Figure 1a), raising the question of whether there is genetic structure among populations. To address this question, we first conducted a principal component analysis in R version 3.3.1 (R Development Core Team, 2016) using the package 'adegenet' using all SNPs (post filtering).

We then tested for the relative explanatory power of IBD versus population genetic structure due to geographical or other barriers

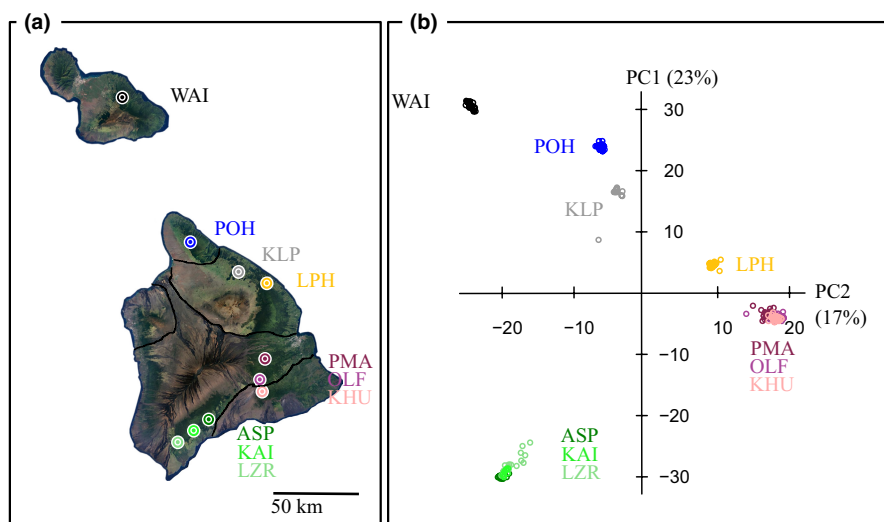


FIGURE 1 Population structure in *Laupala cerasina*. (a) Sampling locations on Maui and Hawai'i (see (b) for colour codes). (b) Principal component analysis on genome-wide SNP data. ASP, *L. cerasina* Alili Spring; KAI, *L. cerasina* Kaiholena; KHU, *L. cerasina* Kahauale'a; KLP, *L. cerasina* Kalopa Park; LPH, *L. cerasina* Laupahoehoe; LZR, *L. cerasina* Lorenzo Rd; OLF, *L. cerasina* Ola'a Forest; PMA, *L. cerasina* Pu'u Maka'ala; POH, *L. cerasina* Ponoholo; WAI, *Laupala waikemoi*.

among populations. Discrete sampling of individuals from a continuously distributed population can result in the false-positive inference of population structure (Meirmans, 2012). Observations of contemporary populations indicate a discrete distribution of suitable habitat for *Laupala* and so we asked whether there is a signal of population genetic structure. We tested for genetic signatures of population structure versus IBD through partitioning variance in spatially explicit genetic analysis using redundancy analyses implemented in the R-package 'vegan' 2.6-4. We included longitude/latitude data (Table S1) and population centroids of the first two principal components as predictor variables and population-average allele frequencies as the response variable. We partitioned variance by first fitting a full model (allele_frequencies ~ lon + lat + PC1 + PC2) followed by partial models for IBD (allele_frequencies ~ lon + lat + Condition(PC1 + PC2)) and genetic structure (allele_frequencies ~ PC1 + PC2 + Condition(lat + lon)).

2.4 | Phylogeography

The volcanoes that jointly form the eastern half of Hawai'i Island vary in age roughly linearly along a north-to-south gradient. This may have facilitated stepwise range expansion followed by isolation and divergence in *L. cerasina*. If so, we would expect the topology of the *L. cerasina* population tree to map to volcano age in the same way that the *Laupala* species topology maps to sequential island ages of the Hawaiian archipelago (Mendelson & Shaw, 2005; Shaw & Gillespie, 2016). Alternatively, population genetic history may be independent of the ages of the Big Island volcanoes, for example, when genetic history is influenced by extinction-recolonisation dynamics due to volcanic eruptions or the result of multiple colonisations.

We used the multispecies coalescent (MSC) model to infer the phylogenetic relationships among *L. cerasina* populations. We asked whether the topology conforms to expectation under the progression rule (Figure 2a). We converted our VCF file with the 2797 SNPs that were called against the pseudo-molecule assembly (Blankers, Oh, Bombarely, et al., 2018) to nexus format file with IUPAC ambiguity coding using a custom R-script. We used PAUP v4.0a164 to perform MSC analysis using the SVDquartets algorithm. We analysed all possible quartets, setting 'handling of ambiguities' to 'distribute' (i.e. interpreting ambiguities as heterozygous sites), and performed 1000 bootstrap replicates. We assigned tips to population partitions after checking that individuals from each population formed a monophyletic group. To check whether the topology varied by genomic region, we also partitioned the VCF file by chromosome and ran SVDquartets on each chromosome separately (see Figure S1 for number of sites per chromosome).

We then generated a time-calibrated phylogeny to infer the timeline of population divergences. We followed the approach taken by Stange et al. (2018) using SNAPP in BEAST v2.4.3 (Bouckaert et al., 2014; Bryant et al., 2012); see also https://github.com/mmatschiner/tutorials/blob/master/divergence_time_estimation_with_snp_data. To accommodate computational restrictions, we selected

three individuals per population that had the least missing sequence data and the highest overall genotype quality scores. Rerunning the MSC analysis in PAUP resulted in the same population topology with the reduced set of three individuals per population (4155 SNPs), compared to the full (4794 SNPs), data set. For SNAPP, we then set a log-normal prior with mean (in real space) equal to 0.5 million years ago (mya) and standard deviation equal to 0.2 Mya to constrain the stem of the divergence between *L. waikemoi* and all *L. cerasina* populations. This incorporates information on likely maximum island age (Blay & Siemers, 2004), as well as uncertainty around phylogenetic time calibration points based on volcanic island age (Forest, 2009). Our analysis thus assumes that *L. cerasina* colonised Hawai'i island around the same time as the emergence of Kohala, but the high standard deviation allows for a broad prior distribution to incorporate uncertainty associated with this assumption. We performed two independent analyses, incorporating one or the other of the two most common alternative topologies (see Section 3). The XML file for BEAST was generated using the `snapp_prep.rb` script (https://raw.githubusercontent.com/mmatschiner/snapp_prep/master/). We then ran SNAPP with a chain length of 1 million samples, deleting the first 100,000 as burn-in.

2.5 | Demographic history

We first tested whether the populations show evidence for historical variation in effective size using Stairway plot v2.1.1 (Liu & Fu, 2020). We converted the full set of SNPs to allele counts and polarised using *L. waikemoi* alleles as ancestral. We then estimated the derived (unfolded, unpolarised) one-dimensional site frequency spectrum (SFS) for each separate population using $\delta\text{a}\delta\text{i}$ (Gutenkunst et al., 2009). We incorporated the one-population SFS in the input file for Stairway plot and ran Stairway plot using 2/3 of the sites for training and four numbers of random break points for each try (1/4, 1/2, 2/3 and 1 times the number of samples in each population). The mutation rate was set at 2.9×10^{-9} , which is the mutation rate estimated for *Heliconius melpomene* (Keightley et al., 2015). From the 1D SFSs, we also calculated F_{ST} , Tajima's D , and Nei's π in $\delta\text{a}\delta\text{i}$. Nei's π was divided by the average length of sequencing reads to approximate a per site estimate.

We then asked whether contemporary populations show evidence for introgression using the ABBA-BABA test (Green et al., 2010; Patterson et al., 2012). Using *L. waikemoi* as an outgroup, we asked whether the test-statistic, D , was significantly higher or lower than zero for all possible combinations of three populations {{P1,P2},P3}, thus providing evidence for gene flow between P1 and P3 or P2 and P3 respectively. We adapted the code from <http://evomics.org/learning/population-and-speciation-genomics/2018-population-and-speciation-genomics/abba-baba-statistics/> and estimated the standard deviation of D by jackknifing over 5MB windows. For this analysis we used the SNPs that mapped to scaffolds assembled into pseudo-molecules (Blankers, Oh, Bombarely, et al., 2018).

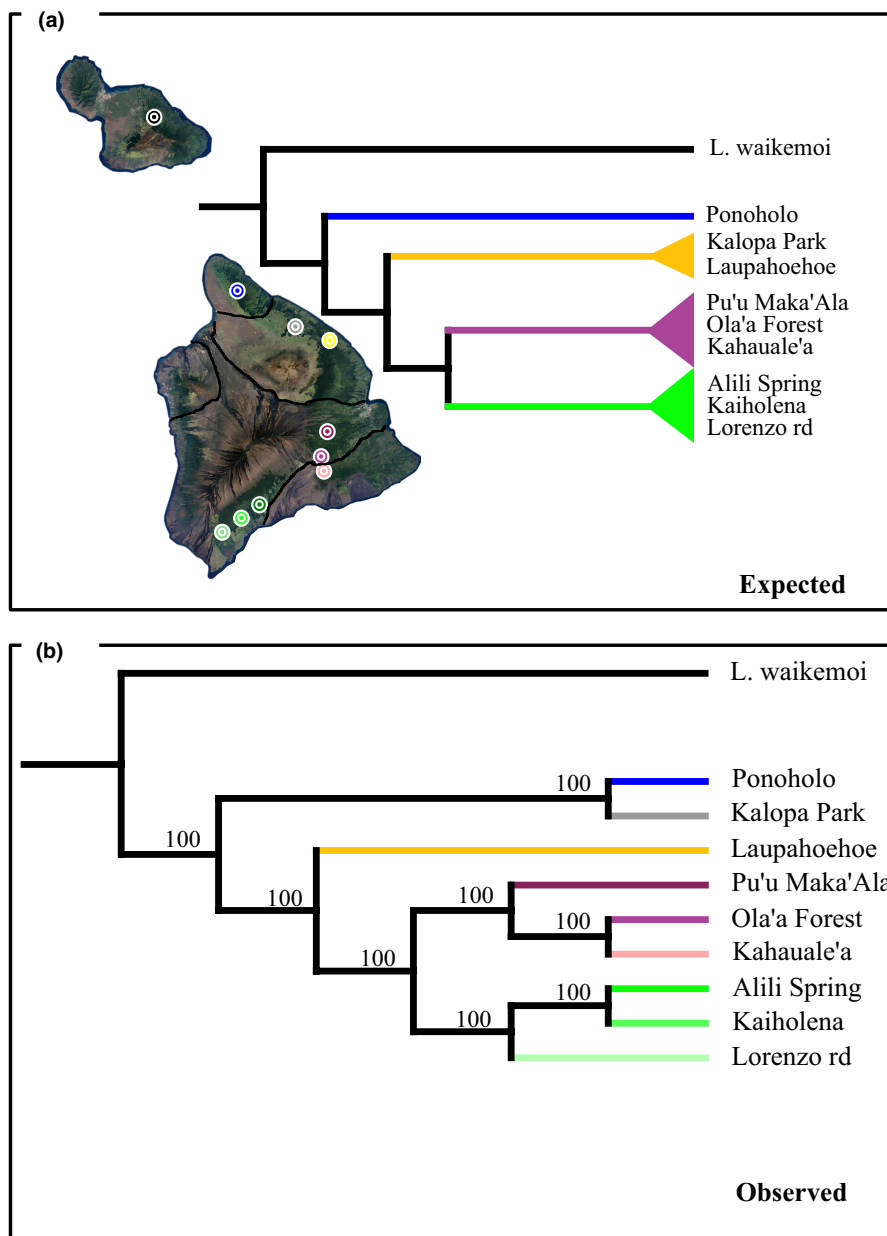


FIGURE 2 Expected (a) and observed (b) outcome of the MSC analysis in SVD quartets. The expectation is based on a progression rule where populations sequentially occupy habitat that arose more recently.

We then used $\delta a\delta i$ (Gutenkunst et al., 2009) to explore the demographic history in more detail, using all SNPs. We created four subsets of the population phylogeny of three populations each: {Ponoholo, Kalopa Park}, Laupahoe and {Laupahoe, {Pu'u Maka'ala, Lorenzo Rd}}, {Pu'u Maka'ala, {Ola'a Forest, Kahauale'a}}, and {Lorenzo Rd, {Kaiholena, Alili Spring}}. For each set of three populations, we generated polarised allele frequency input files (designating *L. waikemoi* alleles as ancestral) from a subset VCF file containing only the three focal populations, excluding sites that were monomorphic in a trio. Within each trio, we then generated all three possible two-dimensional and the three-dimensional site frequency spectra in $\delta a\delta i$. We fitted two-population scenarios for all pairwise combinations that modelled either (asymmetric) migration rates or no migration. We used the insights from the analyses in Stairway plot 2 and of the 2D spectra to inform model

parameterisation and parameter bounds of the more complicated three-population models. For each trio of populations, there are two possible topologies (whether population three splits off from population one or population two) and the populations can have diverged with or without gene flow. We modelled each of these four scenarios for each trio. We first compared the two models with alternative topologies both in the presence and absence of gene flow and then compared the best model without gene flow with the best model with gene flow. We modelled symmetric gene flow, because in the 2D models, most estimates were on the same order of magnitude and associated with high uncertainty (Table S2), suggesting that adding several additional gene flow parameters to the models was not worth the risk of overfitting the model and higher computational demands. Models were compared based on their composite likelihoods if the number of parameters was equal and

using likelihood ratio statistics if they differed in the number of parameters.

Parameter estimates (which are relative to a reference population size and scaled by θ) were obtained from the models with the highest fit and converted to real units (i.e. years, or number of individuals) following the $\delta a\delta i$ manual. The *H. melpomene* mutation rate (Keightley et al., 2015) was used and for sequence length we used the average read length (81.4 bases) times the number of segregating sites in the SFS. Uncertainty in parameter estimates was propagated to calculate standard deviations around the estimates in real units.

2.6 | Patterns of variation in genomic differences along the genome

We asked whether genetic differentiation (estimated using F_{ST}) and divergence (dxy) correlate with (1) recombination rate variation and (2) distance to song QTL across the genome. We projected the recombination landscape (Blankers, Oh, Bombarely, et al., 2018) and seven QTL peaks associated with male song divergence between *L. cerasina* and *L. eukolea* (Blankers, Oh, & Shaw, 2018), a sister species of *L. waikemoi*, onto the pseudo-molecule assembly (Blankers, Oh, Bombarely, et al., 2018) and asked whether variation in levels of F_{ST} and dxy was predicted by variation in recombination and distance to QTL peaks. The analyses were performed using the R package 'PopGenome' (Pfeifer et al., 2014) on the average F_{ST} and dxy across all SNPs in non-overlapping 5MB windows, contrasting all 36 pairs of the nine populations. We then tested whether the time since divergence between population pairs was associated with the correlation between F_{ST} or dxy and recombination rate or distance to a QTL peak. For time-since-divergence we used the estimated mean divergence times from the analysis in SNAPP described above. Because this approach suffers from phylogenetic non-independence of the 36 contrasts (Felsenstein, 1985), we restricted the analysis to the 10 phylogenetically independent contrasts to test the effect of

divergence time on the magnitude and direction of the relationship between genetic/genomic architecture and genetic differentiation/divergence.

3 | RESULTS

3.1 | Strong population structure at small spatio-temporal scales

The PCA revealed strong clustering of individuals by sampling location across *L. cerasina* populations, with the first two principal components explaining 40% of the genetic variation (Figure 1). The genetic clustering by geography resulted in a striking pattern where the sampling locations on Hawai'i Island were approximately recovered in two-dimensional PCA space constrained by the allele frequencies across the 4794 SNPs. Deep levels of genetic differentiation were found at modest geographical distances (Figure 1, Table 1). For example, Ponoeholo is just over 30km away from Kalopa park and about 50km from Laupahoehoe, yet genome-wide F_{ST} estimates are 0.45 and 0.54 respectively (Table 1).

3.2 | Confounded effects from population structure and IBD on genetic variation

To test whether population structure emerges from discrete sampling of a hypothetically continuous *L. cerasina* population subject to IBD, we partitioned variance in allele frequencies among populations (excluding *L. waikemoi*) between effects from space (latitude/longitude) and genetic structure (first two PCs describing population-level variance in allele frequencies). Effects from IBD and genetic structure are confounded, but each also independently contributes variance: 13% of the total variance from IBD and 21% from genetic structure (Table 2).

TABLE 1 Sampling and genetic diversity summary statistics for the nine *L. cerasina* populations.

| Population | Volcano: age (ka) ^a | Sample size | Intraspecific F_{ST} ^b | Interspecific F_{ST} ^b | π ^c | Tajima's D ^c |
|---------------------|--------------------------------|-------------|-------------------------------------|-------------------------------------|--------------------|---------------------------|
| Ponoholo (POH) | Kohala: 430 | 22 | – | 0.65 | 0.00382 ± 0.00006 | 1.16 ± 0.09 |
| Kalopa Park (KLP) | Mauna Kea: 380 | 11 | 0.45 | 0.60 | 0.00345 ± 0.00008 | 0.06 ± 0.07 |
| Laupahoehoe (LPH) | Mauna Kea: 380 | 20 | 0.54 | 0.62 | 0.00354 ± 0.00006 | 0.70 ± 0.07 |
| Pu'u Maka'ala (PMA) | Mauna Loa: 200 | 25 | 0.59 | 0.61 | 0.00334 ± 0.00005 | 0.37 ± 0.07 |
| Ola'a Forest (OLF) | Mauna Loa: 200 | 22 | 0.59 | 0.62 | 0.00353 ± 0.00004 | 0.60 ± 0.06 |
| Kahauale'a (KHU) | Kilauea: 100 | 22 | 0.60 | 0.63 | 0.00353 ± 0.00005 | 0.58 ± 0.07 |
| Lorenzo Rd. (LZR) | Mauna Loa: 200 | 18 | 0.71 | 0.69 | 0.00357 ± 0.00007 | 0.80 ± 0.09 |
| Alili Spring (ASP) | Mauna Loa: 200 | 16 | 0.73 | 0.69 | 0.00373 ± 0.00007 | 0.90 ± 0.08 |
| Kaiholena (KAI) | Mauna Loa: 200 | 8 | 0.70 | 0.72 | 0.00432 ± 0.00007 | 0.79 ± 0.07 |

^aVolcano ages from Roderick et al. (2012).

^b F_{ST} between focal population and (a) Ponoeholo or (b) *L. waikemoi*.

^cStatistics are given as mean ± standard deviation.

TABLE 2 Redundancy analysis to partition variance among geography (IBD) and genetic structure (first two genetic principal components). The first three lines specify the full model (AF = allele frequency, lat = latitude, lon = longitude, PC1 and PC2 are the first two genetic principal components), and the conditional models respectively. The last three lines specify confounded, unexplained and total inertia/variance.

| Model/source | Inertia | R ² | p-Value | % Variance explained | % Total variance |
|---------------------------------------|---------|----------------|---------|----------------------|------------------|
| AF ~ lat + lon + PC1 + PC2 | 45.02 | .77 | .0010 | 1.00 | 0.89 |
| AF ~ lat + lon + Condition(PC1 + PC2) | 6.62 | .10 | .0240 | 0.15 | 0.13 |
| AF ~ PC1 + PC2 + Condition(lat + lon) | 10.58 | .20 | .0030 | 0.24 | 0.21 |
| Confounded | 27.82 | | | 0.62 | 0.55 |
| Unexplained | 5.82 | | | | 0.11 |
| Total | 50.84 | | | | |

3.3 | *L. cerasina* population phylogeography is concordant with the progression rule

The general pattern of population divergence corresponds to the geologic age of the volcanoes (Figure 2). Ponoholo is the basal lineage, located within the geographical confines of the oldest volcano, Kohala (~430ka). The Laupahoehoe population resides within the second oldest volcano, Mauna Kea (~380ka). Divergences among most remaining clades (Pu'u Maka'ala and Ola'a Forest; Lorenzo Road, Kaiholena and Alili Spring), occurred more recently and correspond to the younger age of Mauna Loa (~200ka). The split giving rise to the only population sampled on Kilauea (100ka) is one of the two most recent branching events. A minor anomaly is that the Kalopa Park population appears as the sister group to Ponoholo rather than forming a separate lineage or a closer relationship with Laupahoehoe.

The topology of the tree varied across the genome (Figure S1). Across the eight chromosome specific trees (seven autosomes and the X chromosome), the most notable variation is in the position of the Laupahoehoe population. This population is either placed ancestral to all populations south of Laupahoehoe or in a group with Pu'u Maka'ala, Ola'a Forest, and Kahauale'a that is paraphyletic to Alili Spring, Kaiholena, and Lorenzo Road populations (Figure S1).

Divergence time estimates suggested that most populations were present shortly after the volcano substrates were available for colonisation. Specifically, the mean estimated node ages for (i) the split between {Ponoholo, Kalopa Park} and all other populations, (ii) the split between Laupahoehoe and all other populations, and (iii) the split between {Pu'u Maka'ala, {Ola'a Forest, Kahauale'a}} and {Lorenzo Road, {Alili Spring, Kaiholena}} match closely to the estimated ages for Mauna Kea and Mauna Loa (Figure 3, Figure S2). However, we note the sizeable confidence intervals around these estimates.

3.4 | Population contraction, but no recovery and gene flow among older but not younger populations

Using Stairway plot 2v2.1.1 to reconstruct effective population size through time for each population separately, we found evidence for decreasing population sizes over time for nearly all populations throughout the last 100,000 years (Figure S3). The ABBA-BABA

tests provided evidence for introgression between more highly diverged populations but not between more recently diverged populations. The ABBA-BABA statistic supports significant introgression between Ponoholo and Laupahoehoe, between Kalopa Park and Ponoholo/Laupahoehoe and between Laupahoehoe and Pu'u Maka'ala but not between any other populations (Figure S4). Two-population analyses in $\delta a \delta i$ were used to test for gene flow among pairs of populations and to test whether gene flow was symmetrical among the populations. The two-population analyses supported models with gene flow over models without gene flow for all pairs of populations, except for all three pairs of the trio {Lorenzo Rd, Alili Spring, Kaiholena} and between Pu'u Maka'ala and Kahauale'a (Table S2). In most cases, reciprocal gene flow estimates between pairs were on the same order of magnitude and standard deviations for the migration rate parameters were high ($SD > \text{mean}$).

For the trio {Ponoholo, Kalopa Park, Laupahoehoe}, the best supported model had gene flow between both pairs, population contraction in Laupahoehoe, and Kalopa park splitting off from Ponoholo (Figure 4, Figure S5). For {Laupahoehoe, Pu'u Maka'ala, Lorenzo Rd}, the best model supported gene flow between both pairs, population contraction in Laupahoehoe, and Lorenzo Rd splitting off from Pu'u Maka'ala. For {Pu'u Maka'ala, Ola'a Forest, Kahauale'a}, the best supported model had no gene flow and Kahauale'a splitting off from Ola'a Forest (Figure 4, Figure S5). Lastly, for {Lorenzo Rd, Alili Springs, Kaiholena}, the best supported model had no gene flow and Kaiholena splitting off from Alili Springs (Figure 4, Figure S5).

Divergence time estimates between Ponoholo and Laupahoehoe and between Laupahoehoe and Pu'u Maka'ala were around 300k years, while Pu'u Maka'ala and Ola'a Forest and Lorenzo Rd and Alili Springs were estimated to have diverged less than 10k years ago (Figure 4, Table S3). Despite the support for gene flow models over no-gene flow models in both two-population and three-population analyses, the estimated mean migration rates were very low (~one migrant per 1 million resident individuals per generation) and associated with high standard deviations (Table S3). These models also revealed that unsampled ancestral population size estimates were higher than extant population size estimates and that the magnitude of this difference was higher in older compared to younger trios of extant populations (Table S3).

FIGURE 3 Time-calibrated population divergence. Node values represent divergence time estimates in million years. The only calibration point used was the surfacing age of Hawai'i (around 0.5 Mya) which translated to a log-normal prior with mean 0.5 and standard deviation 0.2 on the *L. cerasina* stem. All branches are supported by Bayes factor = 1.0. Numbers next to the node indicate mean age (in million years). Blue bars indicate 95% Highest Posterior Density. The inset map on the bottom left shows sampling locations, approximate present-day boundaries of the volcanoes, and estimated time of emergence above sea level (in million years ago [Mya]). See Figure S2 for the divergence time estimates when fixing the topology differently.

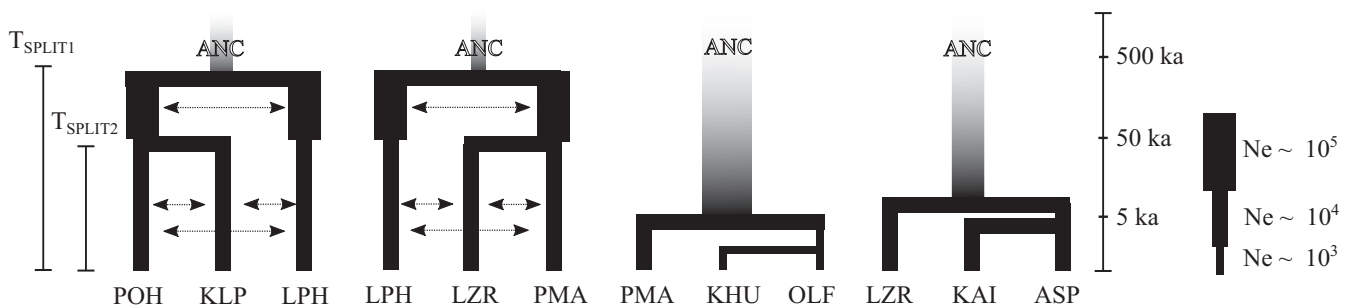
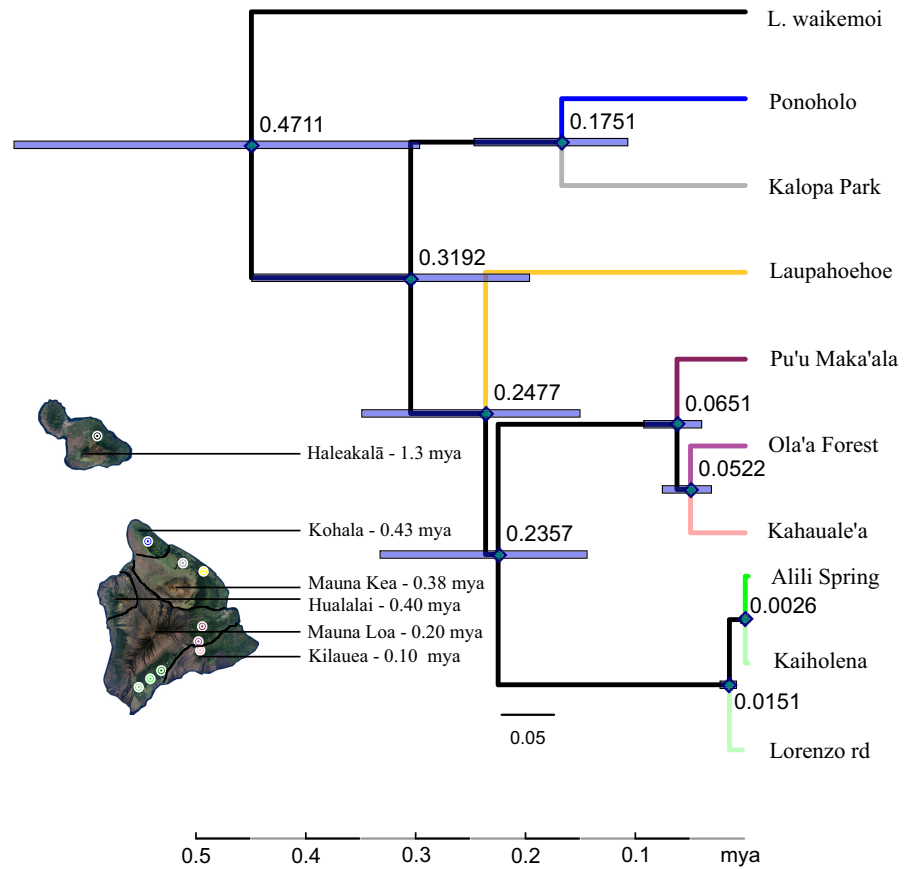


FIGURE 4 Best supported three-population demographic models in $\delta a\delta i$. Horizontal arrows indicate gene flow, which was always modelled as symmetric gene flow that was allowed to differ between before and after T_{split2} . Population contraction is shown as a decrease in the width of the branch. The relative width of the (unsampled) ancestral populations illustrates the ancestral population size inferred for the different models. The width of the bar and the timescale is not to scale and only illustrates relative population sizes and approximate divergence times, as per the legend to the right. See Table S3 for parameter estimates.

3.5 | Patterns of genomic differentiation depend on genomic and genetic architecture

Analysis of the data support the hypothesis of an overall negative correlation between genome-wide variation in F_{ST} and genome-wide variation in recombination rate (Figure 5a, Table S4, note that all correlation coefficients are negative), where F_{ST} is higher in regions of low recombination. The effect size of this correlation appears to increase with increasing divergence time between the populations. In contrast, the correlation between dxy and recombination rate across the genome was positive and its magnitude inversely dependent

on divergence time (Figure 5b, Table S4). Genetic diversity (Nei's π) was positively associated with recombination rate in all populations (Table S6).

Some but not all population pairs showed significant correlations between genetic differentiation (F_{ST}), as well as divergence (dxy), in a genomic window and the distance of the window midpoint to the nearest of seven QTL peaks associated with interspecific song differences (Table S4). Significant correlations were limited to those two (F_{ST}) or three (dxy) contrasts involving the three southern-most (and most recently diverged) populations (Table S4). Across the phylogenetically independent contrasts, the correlation coefficients

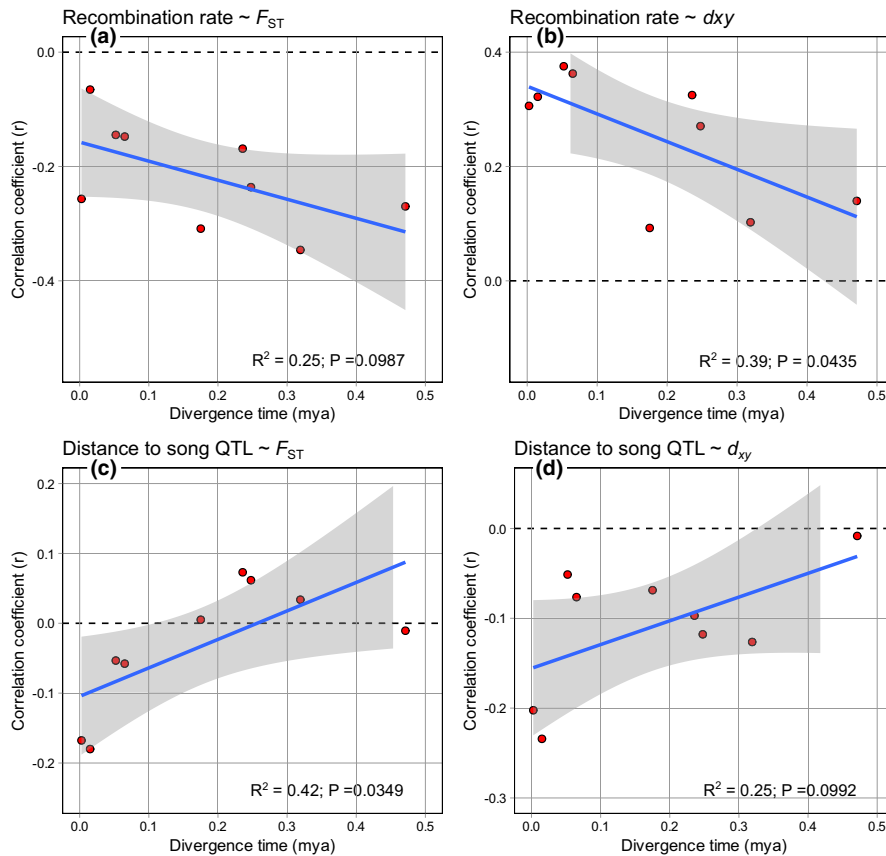


FIGURE 5 The relationship between F_{ST} , d_{xy} , recombination rate (cM/Mb), and distance to a QTL (bp distance between window midpoint and QTL peak position) for song divergence as a function of estimated time since divergence (in million years ago). Each plot shows the relationship between the estimated divergence time for the 10 phylogenetically independent contrasts and the coefficient of the correlation between (a) recombination rate and d_{xy} , (b) recombination rate and F_{ST} , (c) distance to a song QTL peak and F_{ST} , and (d) distance to a song QTL peak and d_{xy} , calculated across the 5 MB genomic windows. The blue line and grey shading show the linear relationship (fit statistics in bottom right corner of each panel) between the correlation coefficient and divergence time.

| | Recombination rate | Song QTL |
|----------|--|--|
| F_{ST} | F_{ST} tends to be <i>higher</i> in regions with <i>reduced</i> recombination in <i>more</i> divergent contrasts | F_{ST} tends to be <i>higher</i> in regions <i>closer</i> to song QTL in <i>less</i> divergent contrasts |
| d_{xy} | d_{xy} tends to be <i>higher</i> in regions with <i>increased</i> recombination in <i>less</i> divergent contrasts | d_{xy} tends to be <i>higher</i> in regions <i>closer</i> to song QTL in <i>less</i> divergent contrasts |

TABLE 3 Summary of the patterns of genetic differentiation in relation to recombination rate and distance to QTL.

tended to become more negative in contrasts with more recent divergence times, indicating that F_{ST}/d_{xy} is higher closer to song QTL in less divergent pairs relative to more divergent pairs (Figure 5, Table 3). In the younger (more recently diverged) populations, but not in the older populations, genetic diversity is also higher closer to song QTL (Table S5).

4 | DISCUSSION

The hidden evolutionary processes fuelling cryptic species diversity (Struck et al., 2018) contribute significantly to the total diversity of life (Czekanski-Moir & Rundell, 2019) and their study is necessary to balance our understanding of the speciation process. Recent work on phenotypic and genomic divergence points to a multitude of factors that influence the evolution of reproductive barriers and shape evolutionary outcomes of speciation in adaptive radiations under ecological selection. We expect that speciation in non-adaptive radiations will likewise share many of these genomic and demographic

factors, despite exhibiting a process of divergence unrelated to ecology (such as may occur due to sexual trait differentiation). It is unknown whether the genomic effects of non-ecological selection may play out differently when, for example, sexual selection acts early and in the absence of ecological selection. Contrasts along the speciation continuum are notably absent for such non-adaptive radiations, especially among cryptic species. Here, we investigated the contribution of biogeographic and evolutionary processes to putative incipient speciation in *Laupala cerasina*, a swordtail cricket endemic to Hawai'i Island.

4.1 | Biogeography

We found that the nine populations that we sampled showed striking population genetic structure at small spatio-temporal scales (Figure 1), with populations placed across a highly supported population-level phylogeny (Figure 2). The rapid and extensive differentiation among populations (this study) and species (Mendelson & Shaw, 2005) of

Laupala does not fit the prediction that allopatric, non-adaptive divergence occurs slowly (Czekanski-Moir & Rundell, 2019). Rather, it shows that neither a specific geographical context (with or without gene flow) nor ecological opportunity is an exclusive predictor of rapid divergence at the population or species level. This is in line with recent work on evolutionary radiations beyond those characterised by ecological opportunity and gene flow (Kagawa, 2022; Martin & Richards, 2019; Matsubayashi & Yamaguchi, 2022; Simões et al., 2016).

The highly supported population phylogeny and associated time estimates of nodal splits (time-calibrated analyses in SNAPP; Figure 3) suggest that the *L. cerasina* lineage arrived on the Big Island sometime prior to 320ka. The uncalibrated divergence time estimates from the $\delta a\delta i$ analysis agree very well with this conclusion (Figure 4, Table S3). The concordance between phylogenetic topology and volcano chronosequence, that is, between estimated divergence times of nodes across the tree and volcano ages (Figure 3, Table S3), favour a subsequent progression from older (300–500 ka) to younger (<100ka) volcanic landscapes, with the oldest split leading to the separation between Ponooho (Kohala) and Kalopa Park (northern Mauna Kea) and the Laupahoehoe population further to the south (Mauna Kea) dating to within the older age of Mauna Kea (380ka). Relatively rapid splits then separate this northern extent of *L. cerasina*, from the two distinct clades on the north-eastern and south-western slopes of Mauna Loa (200ka), nodes that date to 250–240ka; this rapid succession of lineage splitting resulting in incomplete lineage sorting, in combination with gene flow among populations on older volcanoes (Figure 4), is perhaps the reason for an uncertain placement of the Laupahoehoe population as the sister population to the south-eastern clade (Pu'u Maka'ala, Ola'a Forest and Kahauale'a) versus all southerly populations (Figure S1). Thus, the data and above-mentioned analyses argue for a relatively ancient, and in some cases rapid, spread of the *L. cerasina* lineage across the eastern and southern half of Hawai'i Island, coupled with major evolutionary forces of population fragmentation.

Within the context of these broad geographical patterns, the combination of spatially explicit genetic analyses, classical population genetics and demographic modelling reveals a complex history with multiple biogeographic mechanisms at play. First, we show overall high levels of genetic differentiation (Table 1, Figure 1) that are better explained by population structure than geographical distance (Table 2) and little evidence of gene flow broadly connecting subpopulations (Figure 4, Figure S4). This pattern cannot be fully explained by a scenario of isolation-by-distance among well-connected populations. Moreover, extinction re-colonisation seems an unlikely scenario for most of the populations, as we did not find evidence for either bottlenecks or homogenisation of populations inhabiting older, inactive volcanoes; although, recently established populations inhabiting regions with active lava flows may well experience regular replacement.

A history of progression coupled with a scenario of serial founder events has appealed to prior researchers as an explanation of high levels of biodiversity in Hawaii (see Hembry et al., 2021). While our analyses do support progression, we observe overall signals

of population contraction without recovery, as estimated in both $\delta a\delta i$ and Stairway plot demographic analyses (Figure 4, Table S3, Figure S3). Concordantly, populations found on older volcanoes and ancestors of populations found on younger volcanoes were inferred to be larger than contemporary populations on younger volcanoes (Figure 4). Given the timing of these signatures of contraction, beginning approximately 100ka, the results suggest that multiple lineages of *L. cerasina* experienced parallel contraction as their existence predates this signature. Commensurate with these signatures of contraction, we also observed uniformly positive values for Tajima's *D* across these populations (Table 1), indicating more heterozygosity than expected based on nucleotide diversity in the population, a signal that is expected under population contraction (Tajima, 1989). Interestingly, the historical demography estimates in *L. cerasina* mirror the population dynamics in *Metrosideros* species (Izuno et al., 2022) that characterise the *Laupala* habitat and suggests an important role of late Quaternary climate dynamics in combination with the subsidence of aging volcanoes in shaping both rainforest and *Laupala* population dynamics.

These insights lend credence to a history of gradual expansion across younger volcanic substrates when new volcanoes arise, followed by genetic fragmentation as these volcanoes age and subside (causing habitat fragmentation due to erosional forces and/or elevational changes in climate). We acknowledge, however, that both serial founder events and expansion-fragmentation scenarios are similarly dependent on a sequence of geological events: rising volcanoes supporting chance dispersal on the one hand and a chronosequence of erosional fragmentation on the other. Both mechanisms operate under temporally variable availability and connectedness of *L. cerasina* habitat. Most likely, given the complex Hawaiian landscape and climate dynamics in the last 500,000 years, a mixture of scenarios best describes the evolutionary history of *L. cerasina*. In this context, we note that support for gene flow among more diverged (older) populations is stronger than support for gene flow among less-diverged (younger) populations (Figure 4, Figure S4), a pattern that is also consistent with a role for founder events. However, this discrepancy could be a consequence of the overall low rates of gene flow detected, suggesting that longer divergence times favour detection of gene flow signatures in the SFS. We note that, despite agreeing on which populations experience gene flow, estimates for gene flow from the $\delta a\delta i$ models are low compared to the inferred *D* statistic in the ABBA-BABA test. We attribute this inconsistency to the fact that the ABBA-BABA test is sensitive to small population sizes (biased upwardly) and was developed to detect but not to quantify gene flow (Martin et al., 2015).

4.2 | Speciation genomics

While the contribution of phylogeographic and demographic history to overall levels of population differentiation are thus substantial, we also found that genomes have not diverged uniformly across populations. Our results support the influence of two genomic factors,

the recombination landscape and the genetic architecture of sexual communication divergence, on these heterogeneous patterns of divergence. First, we found that levels of differentiation are higher, and thus have increased more rapidly, in genomic regions with low compared to high recombination (Figure 5). Divergence heterogeneity arising from recombination rate variation across the genome is suggestive of a role for background selection (Burri, 2017; Cutter & Payseur, 2013). In these analyses we again uncover a clear signature of the time since divergence between the populations on the relationships among F_{ST} , d_{xy} and recombination rate variation. In all cases there is a negative correlation between F_{ST} and recombination rate and that relationship is stronger for more distantly related pairs of species/populations. Interestingly, these patterns are concordant between this study and, for example, recent work on an adaptive radiation with high gene flow in monkeyflowers (Stankowski et al., 2019) and flycatchers (Burri et al., 2015), in addition to ecological divergence between sunflower species across different geographical contexts (Renaut et al., 2013). The uniformity of these relationships across the taxonomic, geographical and ecological contexts in which divergence took place underlines that recombination rate variation has a strong and evidently universal influence on the genetic divergence process (Burri, 2017; Haenel et al., 2018; Ravinet et al., 2017).

The second source of heterogeneous genomic divergence is linked to a hypothesis of putative speciation genes. In *Laupala*, rapid speciation has been accompanied by divergences in a number of speciation phenotypes, most conspicuously the male mating song (Mendelson & Shaw, 2005). Several genomic regions are known to be involved in song divergence (Blankers et al., 2019; Shaw et al., 2007; Waller et al., 2023), harbouring small-effect alleles that accumulate in confined genomic regions during the process of speciation; moreover, the same genomic regions are involved in multiple independent species divergences (Blankers et al., 2019; Wiley et al., 2012; Xu & Shaw, 2021) and close physical linkage couples male song and female song preference loci (Shaw & Lesnick, 2009; Xu & Shaw, 2019, 2021). The present study revealed, in the most recently diverged population pairs of *L. cerasina*, a significant negative correlation between genetic differentiation/divergence and distance of mating song rhythm QTL known to underlie species differences. Between more divergent population pairs, overall genetic differentiation is higher, which may be swamping the signal of early accentuated differentiation in song QTL regions.

The evolution of sexual signals and preferences across *L. cerasina* populations, which show modest but significant differences in male song and female song preference even among recently diverged populations (Grace & Shaw, 2011), may be causal to or a consequence of population differentiation. Alternatively, song QTL may be in regions of the genome that initially differentiate more rapidly due to mechanisms unrelated to sexual communication behaviour. A third possibility is that these patterns arose by chance, as the only significant associations between F_{ST} and song QTL distance were found in pairs of three related populations in one particular region of Hawai'i.

However, a pattern of increasingly stronger correlations between F_{ST} or d_{xy} and song QTL distance with decreasing divergence time was found across phylogenetically independent contrasts (Figure 5), suggesting it is not driven solely by an idiosyncrasy of the three populations in the south. Increased F_{ST} is not a consequence of reduced diversity in QTL regions as nucleotide diversity is in fact higher in these regions (Table S5). At the same time, if the early accentuated differentiation is no longer detectable in more divergent population pairs, this rules out ongoing divergent selection acting on song QTL beyond the early stages of population divergence. Interestingly, due to widespread linkage of song and preference QTL in *Laupala* (Shaw & Lesnick, 2009; Wiley et al., 2012; Xu & Shaw, 2019) drift and mutation-order processes (or, substitution-order processes in the case of standing genetic variation) could readily result in incomplete reproductive isolation very early on in the divergence history, especially in the context of founder events, and thereby contribute to the genetic structure seen among populations.

Under the premise that our results do not reflect chance, we propose that heterogeneous patterns of genome differentiation can be partly influenced by genetic architecture and by levels of gene flow, both general to adaptive and non-adaptive radiations. Studies that identify associations between phenotype and population differentiation have been most often reported in systems with major effect loci, especially under conditions of high gene flow. Recent examples include the wing colours of mimetic butterflies (Lewis & Reed, 2019) and the nuptial plumage colours of ecologically similar seedeaters (Campagna et al., 2017), where locally accentuated patterns of divergence likely arose due to directional selection in a genomic region harbouring major-effect genes for colour variation, in combination with the homogenising effects of gene flow elsewhere. *Laupala* appears to offer a stark contrast, where high genetic structuring and dispersed, small-effect loci underlying sexual communication behaviour divergence, result in a brief opportunity to detect associations between such loci and elevated patterns of differentiation. It seems unlikely that adaptive radiations will differ systematically from non-adaptive radiations in their degree of genetic structuring (however rapidly generated) or genetic architecture of trait differentiation. This influence of genomic constraint instead suggests another similarity between adaptive and non-adaptive radiations, emphasising general principles of divergence.

In conclusion, by integrating biogeography, population genetics and quantitative genetics in the context of historical geological and climatic dynamics, interesting parallels emerge between the mechanisms driving genomic patterns of divergence among *L. cerasina* populations and genomic divergence among species in various animal and plant radiations. The parallels suggest that distinct modes and mechanisms of speciation (with or without gene flow, adaptive or non-adaptive differentiation) are associated with common core mechanisms. On the background of these shared patterns, we also identify the important role that the selection regime and genetic architecture play in shaping the distribution of genetic divergences and in the resulting diversity in patterns of divergence across taxa in nature. Only when considering complementary approaches and

integrating insights from across disciplines, can we begin to disentangle universal from idiosyncratic mechanisms that drive the speciation process.

AUTHOR CONTRIBUTIONS

T.B. and K.L.S. conceived the study, K.L.S. collected the samples, T.B. analysed the data with input from K.L.S., and T.B. and K.L.S. wrote the paper.

ACKNOWLEDGEMENTS

We thank the Shaw lab members, in particular M. Xu and H. Waller, and other colleagues (P. O'Grady, L. Campagna, R. Gillespie, J. Berv and William D. Gosling) for interesting discussions that have contributed to this manuscript. We also thank J. Lambert for help with sample preparation and L. Campagna for comments on the manuscript. This manuscript further benefited from constructive comments by the editor and three reviewers. This work was supported by the National Science Foundation, grant number DEB1241060: 'Dimensions: Collaborative Research: A Community Level Approach to Understanding Speciation in Hawaiian Lineages'.

CONFLICT OF INTEREST STATEMENT

The authors report no conflict of interest.

DATA AVAILABILITY STATEMENT

Raw genetic data are archived in the short-read archive at NCBI (<https://www.ncbi.nlm.nih.gov/bioproject/PRJNA872373>) and will be made available upon acceptance. All other data and scripts associated with this manuscript are deposited in the Figshare repository (Blankers & Shaw, 2022) and available as supplementary information.

BENEFIT-SHARING STATEMENT

All genetic samples were obtained from within the USA in accordance with national law, with use of required permits, and with respect for local communities and biodiversity.

ORCID

Thomas Blankers  <https://orcid.org/0000-0002-1893-8537>

REFERENCES

- Anderson, S. A. S., & Weir, J. T. (2022). The role of divergent ecological adaptation during allopatric speciation in vertebrates. *Science*, 378, 1214–1218. <https://doi.org/10.1126/science.abo7719>
- Angst, P., Ameline, C., Haag, C. R., Ben-Ami, F., Ebert, D., & Fields, P. D. (2022). Genetic drift shapes the evolution of a highly dynamic metapopulation. *Molecular Biology and Evolution*, 39(12), msac264. <https://doi.org/10.1093/MOLBEV/MSAC264>
- Armstrong, E. E., Perez-Lamarque, B., Bi, K., Chen, C., Becking, L. E., Lim, J. Y., Linderoth, T., Krehenwinkel, H., & Gillespie, R. (2021). A holobiont view of Island biogeography: Unraveling patterns driving the nascent diversification of a Hawaiian spider and its microbial associates. *Molecular Ecology*, 31, 1299–1316. <https://doi.org/10.1111/mec.16301>
- Blankers, T., Oh, K. P., Bombarely, A., & Shaw, K. L. (2018). The genomic architecture of a rapid island radiation: Recombination rate variation, chromosome structure, and genome assembly of the Hawaiian cricket *Laupala*. *Genetics*, 209(4), 1329–1344. <https://doi.org/10.1534/genetics.118.300894>
- Blankers, T., Oh, K. P., & Shaw, K. L. (2018). The genetics of a behavioral speciation phenotype in an island system. *Genes*, 9(7), E346. <https://doi.org/10.1101/250852>
- Blankers, T., Oh, K. P., & Shaw, K. L. (2019). Parallel genomic architecture underlies repeated sexual signal divergence in Hawaiian *Laupala* crickets. *Proceedings of the Royal Society B: Biological Sciences*, 286(1912), 20191479. <https://doi.org/10.1098/rspb.2019.1479>
- Blankers, T., & Shaw, K. L. (2022). Data for: The biogeographic and evolutionary processes shaping population divergence in *Laupala*. <https://doi.org/10.21942/uva.20383980>
- Blay, C., & Siemers, R. (2004). *Kauai's geologic history: A simplified guide*. TEOK Investigations.
- Bouckaert, R., Heled, J., Kühnert, D., Vaughan, T., Wu, C.-H., Xie, D., Suchard, M. A., Rambaut, A., & Drummond, A. J. (2014). BEAST 2: A software platform for Bayesian evolutionary analysis. *PLoS Computational Biology*, 10(4), 1–6. <https://doi.org/10.1371/journal.pcbi.1003537>
- Bryant, D., Bouckaert, R., Felsenstein, J., Rosenberg, N. A., & RoyChoudhury, A. (2012). Inferring species trees directly from Biallelic genetic markers: Bypassing gene trees in a full coalescent analysis. *Molecular Biology and Evolution*, 29(8), 1917–1932. <https://doi.org/10.1093/molbev/mss086>
- Burri, R. (2017). Dissecting differentiation landscapes: A linked selection's perspective. *Journal of Evolutionary Biology*, 30(8), 1501–1505. <https://doi.org/10.1111/jeb.13108>
- Burri, R., Nater, A., Kawakami, T., Mugal, C. F., Olason, P. I., Smeds, L., Suh, A., Dutoit, L., Bures, S., Garamszegi, L. Z., Hogner, S., Moreno, J., Qvarnstrom, A., Ruzic, M., Saether, S. A., Saetre, G. P., Torok, J., & Ellegren, H. (2015). Linked selection and recombination rate variation drive the evolution of the genomic landscape of differentiation across the speciation continuum of *Ficedula flycatchers*. *Genome Research*, 25(11), 1656–1665. <https://doi.org/10.1101/gr.196485.115>
- Campagna, L., Repenning, M., Silveira, L. F., Fontana, C. S., Tubaro, P. L., & Lovette, I. J. (2017). Repeated divergent selection on pigmentation genes in a rapid finch radiation. *Science Advances*, 3(5), e1602404.
- Cotoras, D. D., Bi, K., Brewer, M. S., Lindberg, D. R., Probst, S., & Gillespie, R. G. (2018). Co-occurrence of ecologically similar species of Hawaiian spiders reveals critical early phase of adaptive radiation. *BMC Evolutionary Biology*, 18(1), 1–13. <https://doi.org/10.1186/s12862-018-1209-y>
- Cutter, A. D., & Payseur, B. A. (2013). Genomic signatures of selection at linked sites: Unifying the disparity among species. *Nature Reviews Genetics*, 14(4), 262–274. <https://doi.org/10.1038/nrg3425>
- Czekanski-Moir, J. E., & Rundell, R. J. (2019). The ecology of nonecological speciation and nonadaptive radiations. *Trends in Ecology and Evolution*, 34(5), 400–415. <https://doi.org/10.1016/j.tree.2019.01.012>
- Danecek, P., Auton, A., Abecasis, G., Albers, C. A., Banks, E., DePristo, M. A., Handsaker, R. E., Lunter, G., Marth, G. T., Sherry, S. T., McVean, G., Durbin, R., & Group, 1000 Genomes Project Analysis. (2011). The variant call format and VCFtools. *Bioinformatics*, 27(15), 2156–2158.
- DePristo, M. A., Banks, E., Poplin, R., Garimella, K. V., Maguire, J. R., Hartl, C., Philippakis, A. A., del Angel, G., Rivas, M. A., Hanna, M., McKenna, A., Fennell, T. J., Kernysky, A. M., Sivachenko, A. Y., Cibulskis, K., Gabriel, S. B., Altshuler, D., & Daly, M. J. (2011). A framework for variation discovery and genotyping using next-generation DNA sequencing data. *Nature Genetics*, 43(5), 491–498.
- Elshire, R. J., Glaubitz, J. C., Sun, Q., Poland, J. A., Kawamoto, K., & Buckler, E. S. (2011). A robust, simple genotyping-by-sequencing (GBS) approach for high diversity species. *PLoS One*, 6, e19379. <https://doi.org/10.1371/journal.pone.0019379>
- Felsenstein, J. (1985). Phylogenies and the comparative method. *The American Naturalist*, 125(1), 1–15.

- Forest, F. (2009). Calibrating the tree of life: Fossils, molecules and evolutionary timescales. *Annals of Botany*, 104(5), 789–794. <https://doi.org/10.1093/aob/mcp192>
- Funk, V. A., & Wagner, W. L. (1995). Biogeographic patterns in the Hawaiian Islands. In W. L. Wagner & V. A. Funk (Eds.), *Hawaiian biogeography: Evolution on a hot spot archipelago*. Smithsonian Institution Press.
- Garrison, E., & Marth, G. (2012). Haplotype-based variant detection from short-read sequencing. ArXiv Preprint ArXiv:1207.3907.
- Gavrilets, S., & Losos, J. B. (2009). Adaptive radiation: Contrasting theory with data. *Science*, 323(5915), 732–737. <https://doi.org/10.1126/science.1157966>
- Gillespie, R. G., Bennett, G. M., De Meester, L., Feder, J. L., Fleischer, R. C., Harmon, L. J., Hendry, A. P., Knoppe, M. L., Mallet, J., Martin, C., Parent, C. E., Patton, A. H., Pfennig, K. S., Rubinoff, D., Schluter, D., Seehausen, O., Shaw, K. L., Stacy, E., Stervander, M., ... Wogan, G. O. U. (2020). Comparing adaptive radiations across space, time, and taxa. *Journal of Heredity*, 111(1), 1–20. <https://doi.org/10.1093/jhered/esz064>
- Grace, J. L., & Shaw, K. L. (2011). Coevolution of male mating signal and female preference during early lineage divergence of the Hawaiian cricket, *Laupala cerasina*. *Evolution*, 65(8), 2184–2196. <https://doi.org/10.1111/j.1558-5646.2011.01278.x>
- Grace, J. L., & Shaw, K. L. (2012). Incipient sexual isolation in *Laupala cerasina*: Females discriminate population-level divergence in acoustic characters. *Current Zoology*, 58(3), 416–425. <https://doi.org/10.1093/czoolo/58.3.416>
- Green, R. E., Krause, J., Briggs, A. W., Maricic, T., Stenzel, U., Kircher, M., Patterson, N., Li, H., Zhai, W., Fritz, M. H.-Y., Hansen, N. F., Durand, E. Y., Malaspina, A.-S., Jensen, J. D., Marques-Bonet, T., Alkan, C., Prüfer, K., Meyer, M., Burbano, H. A., ... Pääbo, S. (2010). A draft sequence of the Neandertal genome. *Science*, 328(5979), 710–722. <https://doi.org/10.1126/science.1188021>
- Gutenkunst, R. N., Hernandez, R. D., Williamson, S. H., & Bustamante, C. D. (2009). Inferring the joint demographic history of multiple populations from multidimensional SNP frequency data. *PLoS Genetics*, 5(10), 1–11. <https://doi.org/10.1371/journal.pgen.1000695>
- Haanel, Q., Laurentino, T. G., Roesti, M., & Berner, D. (2018). Meta-analysis of chromosome-scale crossover rate variation in eukaryotes and its significance to evolutionary genomics. *Molecular Ecology*, 27(11), 2477–2497. <https://doi.org/10.1111/mec.14699>
- Hembry, D. H., Bennett, G., Bess, E., Cooper, I., Jordan, S., Liebherr, J., Magnacca, K. N., Percy, D. M., Polhemus, D. A., Rubinoff, D., Shaw, K. L., & O'grady, P. M. (2021). Insect radiations on islands: Biogeographic pattern and evolutionary process in Hawaiian insects. *The Quarterly Review of Biology*, 96(4), 247–296. <https://doi.org/10.1086/717787>
- Hennig, W. (1966). *Phylogenetic systematics*. University of Illinois Press.
- Hotchkiss, S., & Juvik, J. O. (1999). A late-Quaternary pollen record from Ka'au crater, O'ahu, Hawaii. *Quaternary Research*, 52(1), 115–128. <https://doi.org/10.1006/QRES.1999.2052>
- Izuno, A., Onoda, Y., Amada, G., Kobayashi, K., Mukai, M., Isagi, Y., & Shimizu, K. K. (2022). Demography and selection analysis of the incipient adaptive radiation of a Hawaiian woody species. *PLoS Genetics*, 18(1), e1009987. <https://doi.org/10.1371/JOURNAL.PGEN.1009987>
- Kagawa, K. (2022). Toward a mechanism-based classification of evolutionary radiations. *Population Ecology*, 64(2), 108–118. <https://doi.org/10.1002/1438-390X.12101>
- Keightley, P. D., Pinharanda, A., Ness, R. W., Simpson, F., Dasmahapatra, K. K., Mallet, J., Davey, J. W., & Jiggins, C. D. (2015). Estimation of the spontaneous mutation rate in *Heliconius melpomene*. *Molecular Biology and Evolution*, 32(1), 239–243. <https://doi.org/10.1093/molbev/msu302>
- Kozak, K. H., Weisrock, D. W., & Larson, A. (2006). Rapid lineage accumulation in a non-adaptive radiation: Phylogenetic analysis of diversification rates in eastern North American woodland salamanders (Plethodontidae: Plethodon). *Proceedings of the Royal Society B: Biological Sciences*, 273(1586), 539–546. <https://doi.org/10.1098/rspb.2005.3326>
- Lewis, J. J., & Reed, R. D. (2019). Genome-wide regulatory adaptation shapes population-level genomic landscapes in *Heliconius*. *Molecular Biology and Evolution*, 36(1), 159–173. <https://doi.org/10.1093/molbev/msy209>
- Liu, X., & Fu, Y. X. (2020). Stairway Plot 2: Demographic history inference with folded SNP frequency spectra. *Genome Biology*, 21(1), 1–9. <https://doi.org/10.1186/S13059-020-02196-9/FIGURES/2>
- Malinsky, M., Svardal, H., Tyers, A. M., Miska, E. A., Genner, M. J., Turner, G. F., & Durbin, R. (2018). Whole-genome sequences of Malawi cichlids reveal multiple radiations interconnected by gene flow. *Nature Ecology and Evolution*, 2(12), 1940–1955. <https://doi.org/10.1038/s41559-018-0717-x>
- Manichaikul, A., Mychaleckyj, J. C., Rich, S. S., Daly, K., Sale, M., & Chen, W. M. (2010). Robust relationship inference in genome-wide association studies. *Bioinformatics*, 26(22), 2867–2873. <https://doi.org/10.1093/BIOINFORMATICS/BTQ559>
- Marques, D. A., Lucek, K., Meier, J. I., Mwaiko, S., Wagner, C. E., Excoffier, L., & Seehausen, O. (2016). Genomics of rapid incipient speciation in sympatric threespine stickleback. *PLoS Genetics*, 12(2), 1–34. <https://doi.org/10.1371/journal.pgen.1005887>
- Martin, C. H., & Richards, E. J. (2019). The paradox behind the pattern of rapid adaptive radiation: How can the speciation process sustain itself through an early burst? *Annual Review of Ecology, Evolution, and Systematics*, 50, 569–593. <https://doi.org/10.1146/annurev-ecolsys-110617-062443>
- Martin, S. H., Dasmahapatra, K. K., Nadeau, N. J., Salazar, C., Walters, J. R., Simpson, F., Blaxter, M., Manica, A., Mallet, J., & Jiggins, C. D. (2013). Genome-wide evidence for speciation with gene flow in *Heliconius* butterflies. *Genome Research*, 23, 1817–1828. <https://doi.org/10.1101/gr.159426.113>
- Martin, S. H., Davey, J. W., & Jiggins, C. D. (2015). Evaluating the use of ABBA-BABA statistics to locate Introgressed loci. *Molecular Biology and Evolution*, 32(1), 244–257. <https://doi.org/10.1093/molbev/msu269>
- Matsubayashi, K. W., & Yamaguchi, R. (2022). The speciation view: Disentangling multiple causes of adaptive and non-adaptive radiation in terms of speciation. *Population Ecology*, 64(2), 95–107. <https://doi.org/10.1002/1438-390X.12103>
- Matthey-Doret, R., & Whitlock, M. C. (2019). Background selection and FST: Consequences for detecting local adaptation. *Molecular Ecology*, 28(17), 3902–3914. <https://doi.org/10.1111/mec.15197>
- Meier, J. I., Marques, D. A., Mwaiko, S., Wagner, C. E., Excoffier, L., & Seehausen, O. (2017). Ancient hybridization fuels rapid cichlid fish adaptive radiations. *Nature Communications*, 8(1), 14363. <https://doi.org/10.1038/ncomms14363>
- Meirmans, P. G. (2012). The trouble with isolation by distance. *Molecular Ecology*, 21(12), 2839–2846. <https://doi.org/10.1111/j.1365-294X.2012.05578.x>
- Mendelson, T. C., & Shaw, K. L. (2002). Genetic and behavioral components of the cryptic species boundary between *Laupala cerasina* and *L. kohalensis* (Orthoptera: Gryllidae). *Genetica*, 116(2–3), 301–310.
- Mendelson, T. C., & Shaw, K. L. (2005). Rapid speciation in an arthropod. *Nature*, 433, 375–376. <https://doi.org/10.1038/nature03320>
- Mendelson, T. C., Siegel, A. M., & Shaw, K. L. (2004). Testing geographical pathways of speciation in a recent Island radiation. *Molecular Ecology*, 13(12), 3787–3796.
- Nachman, M. W., & Payseur, B. A. (2012). Recombination rate variation and speciation: Theoretical predictions and empirical results from rabbits and mice. *Philosophical Transactions of the Royal Society B: Biological Sciences*, 367(1587), 409–421. <https://doi.org/10.1098/rstb.2011.0249>
- Nosil, P., & Schluter, D. (2011). The genes underlying the process of speciation. *Trends in Ecology and Evolution*, 26(4), 160–167. <https://doi.org/10.1016/j.tree.2011.01.001>

- Otte, D. (1994). *The crickets of Hawaii: Origin, systematics, and evolution*. Orthoptera Society/Academy of Natural Sciences of Philadelphia.
- Pannell, J. R., & Charlesworth, B. (2000). Effects of metapopulation processes on measures of genetic diversity. *Philosophical Transactions of the Royal Society B: Biological Sciences*, 355(1404), 1851–1864. <https://doi.org/10.1098/RSTB.2000.0740>
- Patterson, N., Moorjani, P., Luo, Y., Mallick, S., Rohland, N., Zhan, Y., Genschoreck, T., Webster, T., & Reich, D. (2012). Ancient admixture in human history. *Genetics*, 192(3), 1065–1093. <https://doi.org/10.1534/genetics.112.145037>
- Pfeifer, B., Wittelsbuerger, U., Ramos-Onsins, S. E., & Lercher, M. J. (2014). PopGenome: An efficient Swiss army knife for population genomic analyses in R. *Molecular Biology and Evolution*, 31, 1929–1936. <https://doi.org/10.1093/molbev/msu136>
- Porter, S. C. (2005). Pleistocene snowlines and glaciation of the Hawaiian Islands. *Quaternary International*, 138–139, 118–128. <https://doi.org/10.1016/J.QUAIN.2005.02.009>
- R Development Core Team (2016). *R: A language and environment for statistical computing*. R Foundation for Statistical Computing. (Vol 1, Issue 3.1.2, p. 409). <https://doi.org/10.1007/978-3-540-74686-7>
- Ravinet, M., Faria, R., Butlin, R. K., Galindo, J., Bierne, N., Rafajlović, M., Noor, M. A. F., Mehlig, B., & Westram, A. M. (2017). Interpreting the genomic landscape of speciation: Finding barriers to gene flow. *Journal of Evolutionary Biology*, 30, 1450–1477. <https://doi.org/10.1111/jeb.13047>
- Razkin, O., Sonet, G., Breugelmans, K., Madeira, M. J., Gómez-Moliner, B. J., & Backeljau, T. (2016). Species limits, interspecific hybridization and phylogeny in the cryptic land snail complex *Pyramidula*: The power of RADseq data. *Molecular Phylogenetics and Evolution*, 101, 267–278. <https://doi.org/10.1016/j.ympev.2016.05.002>
- Renaut, S., Grassa, C. J., Yeaman, S., Moyers, B. T., Lai, Z., Kane, N. C., Bowers, J. E., Burke, J. M., & Rieseberg, L. H. (2013). Genomic islands of divergence are not affected by geography of speciation in sunflowers. *Nature Communications*, 4, 1827. <https://doi.org/10.1038/ncomms2833>
- Roderick, G. K., Croucher, P. J. P., Vandergast, A. G., & Gillespie, R. G. (2012). Species differentiation on a dynamic landscape: Shifts in metapopulation genetic structure using the chronology of the Hawaiian Archipelago. *Evolutionary Biology*, 39(2), 192–206. <https://doi.org/10.1007/s11692-012-9184-5>
- Rundell, R. J., & Price, T. D. (2009). Adaptive radiation, nonadaptive radiation, ecological speciation and nonecological speciation. *Trends in Ecology & Evolution*, 24(7), 394–399. <https://doi.org/10.1016/j.tree.2009.02.007>
- Schluter, D. (1996). Ecological causes of adaptive radiation. *The American Naturalist*, 148, S40–S64. <https://doi.org/10.1086/285901>
- Schluter, D. (2000). *The ecology of adaptive radiation*. Oxford University Press.
- Shaw, K. L., & Gillespie, R. G. (2016). Comparative phylogeography of oceanic archipelagos: Hotspots for inferences of evolutionary process. *Proceedings of the National Academy of Sciences of the United States of America*, 113(29), 7986–7993. <https://doi.org/10.1073/pnas.1601078113>
- Shaw, K. L., & Lesnick, S. C. (2009). Genomic linkage of male song and female acoustic preference QTL underlying a rapid species radiation. *Proceedings of the National Academy of Sciences of the United States of America*, 106(24), 9737–9742.
- Shaw, K. L., Parsons, Y. M., & Lesnick, S. C. (2007). QTL analysis of a rapidly evolving speciation phenotype in the Hawaiian cricket *Laupala*. *Molecular Ecology*, 16(14), 2879–2892. <https://doi.org/10.1111/j.1365-294X.2007.03321.x>
- Simões, M., Breitenkreuz, L., Alvarado, M., Baca, S., Cooper, J. C., Heins, L., Herzog, K., & Lieberman, B. S. (2016). The evolving theory of evolutionary radiations. *Trends in Ecology and Evolution*, 31(1), 27–34. <https://doi.org/10.1016/j.tree.2015.10.007>
- Slatkin, M. (1993). Isolation by distance in equilibrium and non-equilibrium populations. *Evolution*, 47(1), 264–279. <https://doi.org/10.2307/2410134>
- Stange, M., Sánchez-Villagra, M. R., Salzburger, W., & Matschner, M. (2018). Bayesian divergence-time estimation with genome-wide single-nucleotide polymorphism data of sea catfishes (Ariidae) supports miocene closure of the Panamanian isthmus. *Systematic Biology*, 67(4), 681–699. <https://doi.org/10.1093/sysbio/syy006>
- Stankowski, S., Chase, M. A., Fuiten, A. M., Rodrigues, M. F., Ralph, P. L., & Streisfeld, M. A. (2019). Widespread selection and gene flow shape the genomic landscape during a radiation of monkeyflow-ers. *PLoS Biology*, 17(7), 1–31. <https://doi.org/10.1371/journal.pbio.3000391>
- Struck, T. H., Feder, J. L., Bendiksbj, M., Birkeland, S., Cerca, J., Gusarov, V. I., Kistenich, S., Larsson, K.-H., Liow, L. H., Nowak, M. D., Stedje, B., Bachmann, L., & Dimitrov, D. (2018). Finding evolutionary processes hidden in cryptic species. *Trends in Ecology & Evolution*, 33(3), 153–163. <https://doi.org/10.1016/j.tree.2017.11.007>
- Tajima, F. (1989). Statistical method for testing the neutral mutation hypothesis by DNA polymorphism. *Genetics*, 123(3), 585–595.
- Toews, D. P. L., Taylor, S. A., Vallender, R., Brelsford, A., Butcher, B. G., Messer, P. W., & Lovette, I. J. (2016). Plumage genes and little else distinguish the genomes of hybridizing warblers. *Current Biology*, 26(17), 2313–2318. <https://doi.org/10.1016/j.cub.2016.06.034>
- Twyford, A. D., Kidner, C. A., & Ennos, R. A. (2015). Maintenance of species boundaries in a Neotropical radiation of *Begonia*. *Molecular Ecology*, 24(19), 4982–4993. <https://doi.org/10.1111/mec.13355>
- Van der Auwera, G. A., Carneiro, M. O., Hartl, C., Poplin, R., del Angel, G., Levy-Moonshine, A., Jordan, T., Shakir, K., Roazen, D., Thibault, J., Banks, E., Garimella, K. V., Altshuler, D., Gabriel, S., & DePristo, M. A. (2013). From FastQ data to high-confidence variant calls: The Genome Analysis Toolkit best practices pipeline. *Current Protocols in Bioinformatics*, 43, 1–11. <https://doi.org/10.1002/0471250953.bi1110s43>
- Waller, H., Blankers, T., Xu, M., & Shaw, K. L. (2023). Quantitative trait loci underlying a speciation phenotype. *Insect Molecular Biology*, 32(6), 592–602. <https://doi.org/10.1111/IMB.12858>
- Wiley, C., Ellison, C. C. K., & Shaw, K. L. K. (2012). Widespread genetic linkage of mating signals and preferences in the Hawaiian cricket *Laupala*. *Proceedings of the Royal Society B: Biological Sciences*, 279, 1203–1209. <https://doi.org/10.1098/rspb.2011.1740>
- Xu, M., & Shaw, K. L. (2019). Genetic coupling of signal and preference facilitates sexual isolation during rapid speciation. *Proceedings of the Royal Society B: Biological Sciences*, 286(1913), 20191607. <https://doi.org/10.1098/rspb.2019.1607>
- Xu, M., & Shaw, K. L. (2021). Extensive linkage and genetic coupling of song and preference loci underlying rapid speciation in *Laupala* crickets. *The Journal of Heredity*, 112(2), 204–213. <https://doi.org/10.1093/jhered/esab001>

SUPPORTING INFORMATION

Additional supporting information can be found online in the Supporting Information section at the end of this article.

How to cite this article: Blankers, T., & Shaw, K. L. (2024). The biogeographic and evolutionary processes shaping population divergence in *Laupala*. *Molecular Ecology*, 33, e17444. <https://doi.org/10.1111/mec.17444>